

COMPACT SCHEMES FOR ADVECTION EQUATION: EMPLOYING INVERSE LAX-WENDROFF PROCEDURE*

KATARÍNA LACKOVÁ[†] AND PETER FROLKOVIČ[‡]

Abstract. Numerical schemes with implicit discretizations in time can offer unconditionally stable numerical methods to solve hyperbolic problems. Such problems can exhibit in general non-smooth solutions; therefore, a careful choice of approximation methods is necessary to avoid unphysical oscillations in numerical solutions. Such approximation techniques are well developed especially for numerical discretizations in space, but it is well known that an additional non-oscillatory approximation is necessary also for the implicit discretization in time when large time steps are used that are not otherwise necessary for explicit methods. In this work, we investigate how one can reach non-oscillatory behavior by incorporating in a numerical scheme the values of the solution evaluated in future time points. Namely, we investigate the inverse Lax-Wendroff procedure to derive such types of scheme and an application of predictor-corrector to implement them in practice. The purpose of this initial study is to evaluate the applicability of this approach to the representative linear advection equation in the 1D case.

Key words. Inverse Lax-Wendroff procedure, linear advection, level set methods

AMS subject classifications. 65M06, 65M12, 35L67

1. Introduction. Consider the following non-conservative advection equation in one-dimensional space:

$$\partial_t \phi + u \partial_x \phi = 0, \quad \phi(x, 0) = \phi^0(x), \quad (1.1)$$

where $\phi = \phi(x, t)$, $x \in [0, \infty)$, $t \in [0, \infty)$ is the unknown function, $u = u(x) > 0$ is given and an inflow Dirichlet boundary condition is prescribed on the left boundary,

$$\phi(0, t) = g(t). \quad (1.2)$$

This equation serves as a solid foundation for testing novel numerical methods for hyperbolic problems. In our case, we are interested in compact implicit numerical schemes that are unconditionally stable and that solve the problem (1.1) and its extension to more general cases. In particular, we are interested in numerical schemes for level set methods [14, 8] in which the advected function ϕ is a continuous function with possible discontinuities in its gradient. If one is also interested in a good approximation of the gradient, a careful choice of approximation techniques is required.

One of such techniques are essentially non-oscillatory (ENO) approximations (and related ones like WENO) that are widely used for numerical solutions of conservation laws [15]. If one denotes $\psi = \partial_x \phi$, the function ψ has to fulfill the conservative advection equation related to (1.1),

$$\partial_t \psi + \partial_x (u\psi) = 0. \quad (1.3)$$

*The work of the first author is supported by the European Union, ESG grant 23-01-04-A, the work of the second one by the grants VEGA 1/0314/23, VEGA 1/0249/24, APVV-19-0460 and APVV-23-0186.

[†]Department of Mathematics and Descriptive Geometry, Slovak University of Technology, Bratislava, Slovakia (katarina.lackova@stuba.sk).

[‡]Department of Mathematics and Descriptive Geometry, Slovak University of Technology, Bratislava, Slovakia (peter.frolkovic@stuba.sk).

Although we are primarily interested in the solution ϕ of (1.1), we relate it to the solution ψ of (1.3) in which a proper numerical approximation of a possibly discontinuous function without artificial oscillations is required.

One particular example of an unconditionally stable numerical scheme to solve (1.1) is the following compact implicit parametric finite difference scheme [8], defined on a regular spatial grid with step size $h := x_{i+1} - x_i$, where $i \in \{0, 1, 2, \dots, I\}$ is the spatial index, and with a uniform time discretization with time step $\tau := t^n - t^{n-1}$ with $n \in \{1, 2, 3, \dots, N\}$ being the time index:

$$\begin{aligned} \Phi_i^n + C_i \left(\Phi_i^n - \Phi_{i-1}^n + \frac{1 - \omega_i^n}{2} (\Phi_{i+1}^{n-1} - \Phi_i^{n-1} - \Phi_i^n + \Phi_{i-1}^n) \right. \\ \left. + \frac{\omega_i^n}{2} (\Phi_i^{n-1} - \Phi_{i-1}^{n-1} - \Phi_{i-1}^n + \Phi_{i-2}^n) \right) = \Phi_i^{n-1}. \end{aligned} \quad (1.4)$$

Here, $C_i := \tau u_i / h$ is a non-dimensional Courant number with $u_i = u(x_i)$ and $\Phi_i^n \approx \phi(x_i, t^n)$. The scheme (1.4) is second order accurate for any value of the parameter ω_i^n and it is unconditionally stable using the von Neumann stability analysis for $C_i > 0$ and $\omega_i^n \geq 0$ [6]. The scheme (1.4) is derived in [8] using the so-called (direct) Lax-Wendroff procedure based on Taylor series. Such tools have recently become popular for deriving implicit numerical schemes [1, 17, 4, 7]. We give here details later on the derivation of an analogous scheme to (1.4) when using the inverse Lax-Wendroff procedure.

REMARK 1. *Note that the stencil in the implicit part of the scheme (1.4) contains only the unknowns in the upwind direction. The values Φ_0^n are given by the boundary conditions (1.2) and to express Φ_1^n one can conveniently use $\omega_1^n = 0$ in (1.4). Consequently, the numerical solution Φ_i^n can be obtained simply by "marching in time" with $n = 1, 2, \dots$ and using a forward substitution when solving (1.4) for $i = 1, 2, \dots$. This approach can also be used in more general settings when applying the so-called fast sweeping method [18] with Gauss-Seidel iterations realized with different orderings of unknowns.*

Note that a related numerical scheme can be defined for the advection equation in the conservative form (1.3). If we denote $\Psi_i^n = \Phi_i^n - \Phi_{i-1}^n \approx h \partial_x \phi(x_i, t^n)$, by the difference of (1.4) for i and $i - 1$, one obtains

$$\begin{aligned} \Psi_i^n + C_i \left(\Psi_i^n + \frac{1 - \omega_i^n}{2} (\Psi_{i+1}^{n-1} - \Psi_i^n) + \frac{\omega_i^n}{2} (\Psi_i^{n-1} - \Psi_{i-1}^n) \right) \\ - C_{i-1} \left(\Psi_{i-1}^n + \frac{1 - \omega_{i-1}^n}{2} (\Psi_i^{n-1} - \Psi_{i-1}^n) + \frac{\omega_{i-1}^n}{2} (\Psi_{i-1}^{n-1} - \Psi_{i-2}^n) \right) = \Psi_i^{n-1}. \end{aligned} \quad (1.5)$$

This scheme resembles a conservative finite difference scheme for the numerical solution of (1.3). As noted above, the function ψ can exhibit discontinuities; therefore, our aim is to choose the values ω_i^n in such a way that the approximation of Ψ is non-oscillatory. The main idea behind this is to define the so-called limiters l_i by

$$l_i = 1 - \omega_i^n + \omega_i^n r_i, \quad r_i = \frac{\Psi_{i-1}^n - \Psi_i^{n-1}}{\Psi_i^n - \Psi_{i+1}^{n-1}}. \quad (1.6)$$

Without going into details, see [8] for the full derivation, to obtain a non-oscillatory behavior of Ψ_i^n , the limiters must fulfill the inequalities;

$$-2 \leq \frac{l_i}{r_i} - l_{i-1} \leq \frac{2}{C_i}. \quad (1.7)$$

It is very important to note that similar inequalities, if $0 < C_i \leq 1$, are well-known requirements when developing a variety of limiters for a general class of numerical methods for hyperbolic problems; see, e.g., [11, 5, 9]. In that case, one can always choose ω_i^n (dependent on the numerical solution Φ_i^n) so that the inequalities are fulfilled [8].

Unfortunately, it cannot be done in general if $C_i > 1$ when such values of parameters ω_i^n need not be available, and an additional “time limiting” must be applied to ensure the non-oscillatory behavior of Ψ_i^n , see [5, 12, 7]. This type of limiting eventually decreases the order of accuracy of (1.4), which may take the form of a first-order accurate scheme for very large Courant numbers. As we are interested in numerical solutions of (1.1) for arbitrary Courant numbers, this is our main motivation to develop numerical schemes analogous to (1.4) that are second-order accurate for any C_i without usage of the first-order accurate time limiting.

REMARK 2. *In the context of selecting the parameter ω_i^n in (1.4) to use a second-order approximation in space, we choose here a WENO approximation [15] and the predictor-corrector method [12]. Firstly, we predict the value Ψ_i^n (that is, Φ_i^n and Φ_{i-1}^n) by the predictors $\Phi_i^{n,p}$ obtained from the first-order implicit numerical scheme,*

$$\Phi_i^{n,p} = (\Phi_i^{n-1} + C_i \Phi_{i-1}^n) / (1 + C_i). \quad (1.8)$$

Having such values, we compute two terms used for the second-order update in (1.4), i.e. for two special choices of the parameter, either $\omega_i^n = 1$ or $\omega_i^n = 0$,

$$\begin{aligned} r_i^{n,u} &= \Psi_i^{n-1} - \Psi_{i-1}^n = \Phi_i^{n-1} - \Phi_{i-1}^{n-1} - \Phi_{i-1}^n + \Phi_{i-2}^n \\ r_i^{n,d} &= \Psi_{i+1}^{n-1} - \Psi_i^{n,p} = \Phi_{i+1}^{n-1} - \Phi_i^{n-1} - \Phi_i^{n,p} + \Phi_{i-1}^{n,p} \end{aligned} \quad (1.9)$$

and

$$\omega_i^n = \frac{\tilde{\omega} ((r_i^{n,u})^2 + \epsilon)^{-2}}{\tilde{\omega} ((r_i^{n,u})^2 + \epsilon)^{-2} + (1 - \tilde{\omega}) ((r_i^{n,d})^2 + \epsilon)^{-2}}, \quad (1.10)$$

where $\tilde{\omega} = 1/3$ is the preferable value of the parameter in the case of smooth solutions. The parameter ϵ is a small value chosen to avoid dividing by zero [15]. Using the value ω_i^n from (1.10) in (1.4), one computes the corrected value of Φ_i^n .

The paper is organized as follows. The inverse compact scheme is derived in Section 2. The scheme can be applied using a marching in space; to use the traditional marching in time, a predictor-corrector form is derived. In Section 3, we combine the direct and the inverse schemes to define a general one that can be used for arbitrary Courant numbers. In Section 4, several numerical experiments are provided to compare the schemes for specific examples. Finally, we conclude in Section 5.

2. Inverse compact scheme. In the previous section, we established the foundation for our discussion by introducing the compact implicit second order scheme (1.4) that has essentially no oscillations in the solution gradient for $C_i \leq 1$ if, e.g., the WENO parameters (1.10) are used.

Let us rewrite the equation (1.1) in the following form:

$$\partial_x \phi + \frac{1}{u} \partial_t \phi = 0, \quad \phi(0, t) = g(t) \quad (2.1)$$

and $\phi(x, 0) = \phi^0(x)$. In this alternative formulation, the exchange of roles between x and t leads to an interesting observation: As velocity u increases, the corresponding

slowness $1/u$ decreases. This inverse relationship highlights the change in our description of propagation speed and will ultimately allow us to define a scheme analogous to (1.4) with (1.10) that is oscillation-free in the gradient for $C_i \geq 1$.

We use the abbreviation for the exact values $\phi_i^n = \phi(x_i, t^n)$, $\partial_x \phi_i^n = \partial_x \phi(x_i, t^n)$, etc. In order to derive a new numerical scheme to solve (2.1), we begin with the Taylor expansion at point (x_{i-1}, t^n) ,

$$\phi_{i-1}^n = \phi_i^n - h \partial_x \phi_i^n + \frac{h^2}{2} \partial_{xx} \phi_i^n + \mathcal{O}(h^3). \quad (2.2)$$

Furthermore, we use the inverse Lax-Wendroff procedure [16] having

$$\partial_x \phi_i^n = -\frac{1}{u_i} \partial_t \phi_i^n \quad (2.3a)$$

$$\partial_{xx} \phi_i^n = -\partial_x \left(\frac{1}{u_i} \partial_t \phi_i^n \right) = -\frac{1}{u_i} \partial_{xt} \phi_i^n + \frac{u_i'}{u_i^2} \partial_t \phi_i^n. \quad (2.3b)$$

Substituting the spatial derivatives in (2.2) by (2.3a) and (2.3b) we have

$$\phi_{i-1}^n = \phi_i^n + \frac{h}{u_i} \partial_t \phi_i^n - \frac{h^2}{2u_i} \partial_{xt} \phi_i^n + \frac{h^2 u_i'}{2u_i^2} \partial_t \phi_i^n + \mathcal{O}(h^3), \quad (2.4)$$

which we further can approximate by appropriate finite differences to obtain the required numerical scheme. To our knowledge, the inverse procedure has not been used up to now for such a purpose, but is very popular otherwise for the treatment of boundary conditions when using high-order numerical schemes [16].

For $u_i > 0$, we choose the following parametric finite difference approximations:

$$\partial_t \phi_i^n \approx \frac{\phi_i^n - \phi_i^{n-1}}{\tau} + \frac{1 - \alpha_i^n}{2\tau} (\phi_i^{n+1} - 2\phi_i^n + \phi_i^{n-1}) + \frac{\alpha_i^n}{2\tau} (\phi_i^n - 2\phi_i^{n-1} + \phi_i^{n-2}), \quad (2.5)$$

$$\partial_{xt} \phi_i^n \approx \frac{1 - \alpha_i^n}{\tau h} (\phi_i^{n+1} - \phi_i^n - \phi_{i-1}^{n+1} + \phi_{i-1}^n) + \frac{\alpha_i^n}{\tau h} (\phi_i^n - \phi_{i-1}^n - \phi_i^{n-1} + \phi_{i-1}^{n-1}), \quad (2.6)$$

where $\alpha_i^n \geq 0$ is a free parameter to choose.

In the case of a variable velocity u , the term $\frac{h^2}{2} \frac{u_i'}{u_i^2} \partial_t \phi_i^n$ is also approximated by a simple backward first-order finite difference. Consequently, we obtain the resulting scheme in the following form for $C_i > 0$:

$$\begin{aligned} \Phi_i^n + C_i (\Phi_i^n - \Phi_{i-1}^n) + \frac{1}{2C_i} (C_i - C_{i-1}) (\Phi_i^n - \Phi_i^{n-1}) \\ + \frac{1 - \alpha_i^n}{2} (\Phi_{i-1}^{n+1} - \Phi_{i-1}^n - \Phi_i^n + \Phi_i^{n-1}) \\ + \frac{\alpha_i^n}{2} (\Phi_{i-1}^n - \Phi_{i-1}^{n-1} - \Phi_i^{n-1} + \Phi_i^{n-2}) = \Phi_i^{n-1}. \end{aligned} \quad (2.7)$$

At this point one can see that choosing the approximation (2.5) and (2.6) in (2.2), the value Φ_i^{n+1} has canceled out and the final scheme includes only the value Φ_{i-1}^{n+1} in the future time point t^{n+1} . Analogously to the direct scheme (1.4), resp. (1.5), to have non-oscillatory approximation for numerical solutions obtained with (2.7), the parameters α_i^n shall fulfill analogous constraints as ω_i^n in (1.7), but now with $C_i \geq 1$. Note that this analogy is valid only for constant velocity.

Similarly as in (1.10), to construct the final second-order WENO scheme, we define α_i^n as follows:

$$\begin{aligned} s_i^u &= \Phi_{i-1}^n - \Phi_{i-1}^{n-1} - \Phi_i^{n-1} + \Phi_i^{n-2} \\ s_i^d &= \Phi_{i-1}^{n+1} - \Phi_{i-1}^n - \Phi_i^{n,p} + \Phi_i^{n-1,p} \\ \alpha_i^n &= \frac{\tilde{\alpha}((s_i^u)^2 + \epsilon)^{-2}}{\tilde{\alpha}((s_i^u)^2 + \epsilon)^{-2} + (1 - \tilde{\alpha})((s_i^d)^2 + \epsilon)^{-2}}, \end{aligned} \quad (2.8)$$

where $\tilde{\alpha} = 1/3$ and the values $\Phi_i^{n,p}, \Phi_i^{n-1,p}$ are first-order predictors identical to (1.8).

Both schemes (1.4) and (2.7) have a compact implicit part of the stencil, and can be solved efficiently using solvers such as the fast sweeping method, see Remark 1. However, they are truly analogous only when the time-marching algorithm ($n = 1, 2, \dots$) to solve the system of linear equations (1.4) is replaced by the space-marching algorithm ($i = 1, 2, \dots$) to solve (2.7).

REMARK 3. *In order to employ the traditional time-marching loop for the inverse scheme (2.7), it is necessary to make use of additional predictors computed as*

$$\bar{\Phi}_{i-1}^{n+1,p} = \left(\Phi_{i-1}^n + C_{i-1} \bar{\Phi}_{i-2}^{n+1,p} \right) / (1 + C_{i-1}). \quad (2.9)$$

The resulting scheme has the following form:

$$\begin{aligned} \Phi_i^n + C_i (\Phi_i^n - \Phi_{i-1}^n) + \frac{1}{2C_i} (C_i - C_{i-1})(\Phi_i^n - \Phi_i^{n-1}) \\ + \frac{1 - \alpha_i^n}{2} \left(\bar{\Phi}_{i-1}^{n+1,p} - \bar{\Phi}_{i-1}^{n,p} - \Phi_i^{n,p} + \Phi_i^{n-1,p} \right) \\ + \frac{\alpha_i^n}{2} (\Phi_{i-1}^n - \Phi_{i-1}^{n-1} - \Phi_i^{n-1} + \Phi_i^{n-2}) = \Phi_i^{n-1}, \end{aligned} \quad (2.10)$$

and α_i^n is computed using (2.8) with

$$s_i^d = \bar{\Phi}_{i-1}^{n+1,p} - \bar{\Phi}_{i-1}^{n,p} - \Phi_i^{n,p} + \Phi_i^{n-1,p}. \quad (2.11)$$

Note that the scheme (2.10) formally contains the values of the numerical solutions at future time points t^{n+1} to compute the value Φ_i^n . Of course, future values must be predicted by (2.9) to be available. An analogous approach is used for the so-called extended backward differentiation formulae in [3] to integrate numerically ordinary differential equations.

An analogous scheme to (2.10) can be used instead of (1.4) where the values $r_i^{n,p}$ are completely computed from first-order predictors analogously to (2.11). In both cases, although the predictors are of first-order accuracy, the numerical experiments showed the schemes are second-order accurate for smooth solutions; see Table 2.1.

3. General high-resolution scheme. So far we have explored the characteristics of two similar numerical schemes: the direct scheme (1.4), typically favored when $C_i \leq 1$, and the inverse scheme (2.7), which is applicable only when $C_i > 0$ and is preferable when $C_i \geq 1$. In order to make use of both in general form, e.g., when the velocity u is not constant, we combine them, making use of predictors as described in Remark 3.

Recall the Courant number, denoted by C_i , as defined earlier in this article. Now, we refine this definition by expressing it as the sum of two components, c_i and d_i ,

I	N	Direct scheme				Inverse scheme			
		E_L^N	EOC	E_∞	EOC	E_L^N	EOC	E_∞	EOC
100	10	1.58E-03		1.84E-03		3.13E-03		5.83E-03	
200	20	3.53E-04	2.16	6.25E-04	1.56	6.20E-04	2.33	2.18E-03	1.42
400	40	8.33E-05	2.08	2.80E-04	1.16	1.27E-04	2.29	7.71E-04	1.50
800	80	1.99E-05	2.07	1.19E-04	1.23	2.52E-05	2.33	2.12E-04	1.86
1600	160	4.90E-06	2.02	3.17E-05	1.91	5.49E-06	2.20	5.40E-05	1.97

TABLE 2.1

Table of accuracy for both the direct and inverse scheme according to Remark 3. In this example, a smooth initial condition $\phi_0(x) = \cos(x)$ was chosen on interval $x \in [-\pi/2, 3\pi/2]$, and a constant velocity $u(x) = 1$ with the Courant number $C_i = 1$. The final time was $T = 1$. More details regarding the numerical solution algorithm can be found in Section 4.

such that $C_i = c_i + d_i$, where $c_i = \min\{C_i, 1\}$ and $d_i = C_i - c_i$. Then the final general second-order scheme has the following form:

$$\begin{aligned}
 & \Phi_i^n + C_i(\Phi_i^n - \Phi_{i-1}^n) + \frac{d_i}{2C_i^2}(C_i - C_{i-1})(\Phi_i^n - \Phi_i^{n-1}) \\
 & \quad + \frac{C_i}{2}(\omega_i^n (\Phi_i^{n-1} - \Phi_{i-1}^{n-1} - \Phi_{i-1}^n + \Phi_{i-2}^n) \\
 & \quad + (1 - \omega_i^n) (\Phi_{i+1}^{n-1} - \Phi_i^{n-1} - \Phi_i^{n,p} + \Phi_{i-1}^{n,p})) \\
 & \quad + \frac{d_i}{2C_i}(\alpha_i^n (\Phi_{i-1}^n - \Phi_{i-1}^{n-1} - \Phi_i^{n-1} + \Phi_i^{n-2}) \\
 & \quad + (1 - \alpha_i^n) (\Phi_{i-1}^{n+1,p} - \Phi_{i-1}^{n,p} - \Phi_i^{n,p} + \Phi_i^{n-1,p})) = \Phi_i^{n-1}
 \end{aligned} \tag{3.1}$$

with ω_i^n and α_i^n from Remark 3.

The schematic representation of the resulting stencil can be seen in Figure 3.1. It is worth remarking on the use of the value Φ_{i-1}^{n+1} at the “future” time point t^{n+1} .

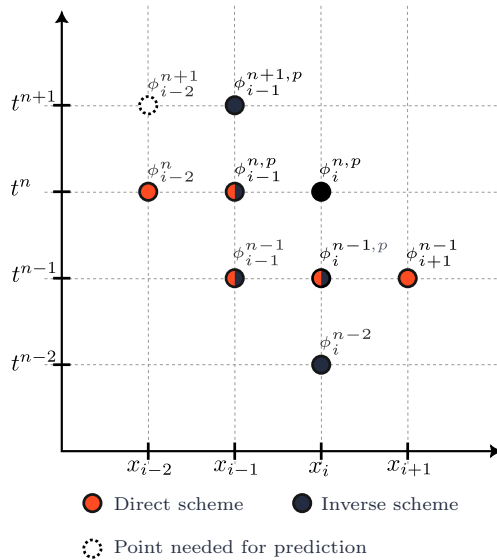


FIG. 3.1. Stencil of the general scheme (3.1) for $u(x) > 0$.

4. Numerical experiments. In the following section, we provide a set of numerical experiments using the numerical schemes described in this paper. In all examples, we use the fast sweeping method to solve the resulting system of linear equations as discussed in Remark 1.

In all the numerical experiments described in this section we use the exact solution in the boundary and initial conditions. Furthermore, we calculate the accuracy of the solution using the norms

$$E_I^N := \tau h \sum_{n=0}^N \sum_{i=0}^I |\Phi_i^n - \phi(x_i, t^n)|, \quad E_\infty := \max_{i,n} |\Phi_i^n - \phi(x_i, t^n)|,$$

with ϕ being the exact solution. The implementation was done in Julia [2].

4.1. Advection with constant velocity. In the following numerical experiment, we solve equation (1.1) with a given constant velocity $u(x) = 1$ and a special periodic exact solution $\phi(x, t)$ whose lengthy definition can be found in [13, 10, 8], consult also the graph of $\phi(x, 1)$ at the top of Figure 4.1. The function $\partial_x \phi(x, t)$ has three moving discontinuities; see the plot of $\partial_x \phi(x, 1)$ at the bottom of Figure 4.1.

The computational domain is $x \in [-1, 1]$ and $t \in [0, 1]$. We compute the solution with the Courant number $C = 3$ and compare the result of two solutions, one obtained using the direct numerical scheme (1.4) with (1.10) and one using the proposed inverse scheme (2.7) with (2.8). For the direct scheme, we use the classical time-marching loop, and for the inverse scheme, a space-marching loop is used, as described in Remark 3. The results can be seen in Figure 4.1 and Table 4.1. Although the direct scheme gives slightly more accurate numerical solutions, it clearly has an oscillatory approximation of its space derivative.

To evaluate this behavior, we compare the accuracy of the space derivative approximation of both numerical solutions in the final time $T = 1$ using the norms $\hat{E}_I := h \sum_{x_i \in \Omega_\delta} |\Psi_i^N - \psi(x_i, t^N)|$ and $\hat{E}_\infty := \max_{x_i \in \Omega_\delta} |\Psi_i^N - \psi(x_i, t^N)|$. Here, Ω_δ is the interval $x \in [-1, 1]$ that excludes small fixed intervals $(\bar{x}_k - 0.02, \bar{x}_k + 0.02)$ for three points \bar{x}_k of discontinuities in $\partial_x \phi(x, 1)$. The results can be found in Table 4.2 where a better accuracy can be clearly observed for the inverse scheme.

		Direct scheme				Inverse scheme			
I	N	E_I^N	EOC	E_∞	EOC	E_I^N	EOC	E_∞	EOC
400	40	4.23E-02		4.86E-01		6.47E-02		7.28E-01	
800	80	1.57E-02	1.43	2.94E-01	0.72	2.05E-02	1.66	4.22E-01	0.79
1600	160	6.12E-03	1.36	1.81E-01	0.70	6.80E-03	1.59	2.46E-01	0.78
3200	320	2.42E-03	1.34	1.12E-01	0.69	2.29E-03	1.57	1.44E-01	0.77

TABLE 4.1

Accuracy results for the numerical approximations of ϕ with non-smooth initial condition and constant velocity computed with the direct scheme (1.4) and the inverse scheme (2.7).

4.2. Advection with variable velocity. Next, we test the proposed general scheme (3.1) on examples with variable velocity.

Firstly, we solve equation (1.1) with $u(x) = 2 + 3/2 \cos(x)$ and with the initial condition given as $\phi_0(x) = \cos(x)$. The exact smooth solution has the following analytical form:

$$\phi(x, t) = \cos \left(2 \arctan \left(\sqrt{7} \tan \left(\sqrt{7} \left(t - \frac{4 \arctan(\tan(x/2)/\sqrt{7})}{\sqrt{7}} \right) / 4 \right) \right) \right).$$

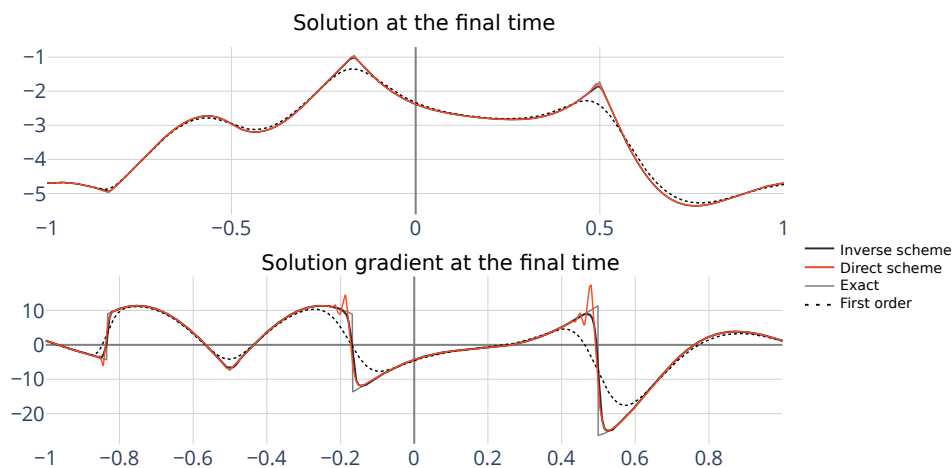


FIG. 4.1. Solutions at the final time $T = 1$ of the advection equation (1.1) with constant velocity and non-smooth initial condition using $I = 3200$ computed with the direct scheme (1.4) and the inverse scheme (2.7). For a comparison, the numerical solution obtained with the first order scheme is also included.

I	N	Direct scheme				Inverse scheme			
		\hat{E}_I	EOC	\hat{E}_∞	EOC	\hat{E}_I	EOC	\hat{E}_∞	EOC
800	80	8.72E-01		12.461		8.90E-01		8.693	
1600	160	4.19E-01	1.06	6.650	0.91	2.73E-01	1.71	4.943	0.81
3200	320	2.09E-01	1.00	7.370	-0.15	7.14E-02	1.93	1.623	1.61
6400	640	7.45E-02	1.49	3.738	0.98	2.31E-02	1.63	5.15E-01	1.66
12800	1280	2.78E-02	1.42	2.163	0.79	9.49E-03	1.28	3.10E-01	0.73

TABLE 4.2

Accuracy results for the numerical approximation of $\psi = \partial_x \phi$ with non-smooth initial condition and constant velocity computed with the direct scheme (1.4) and the inverse scheme (2.7).

The final time was set to $T = \pi/\sqrt{3}$ and the computational domain was $x \in [-\pi/2, 3\pi/2]$. The results of this experiment can be found in Table 4.3 and they confirm the second-order accuracy of the general scheme (3.1) for this example.

I	N	General scheme			
		E_I^N	EOC	E_∞	EOC
100	10	4.87E-02		1.08E-01	
200	20	9.56E-03	2.35	2.20E-02	2.30
400	40	1.83E-03	2.38	4.27E-03	2.36
800	80	3.51E-04	2.39	8.58E-04	2.32
1600	160	7.11E-05	2.30	1.76E-04	2.29

TABLE 4.3

Accuracy results for numerical experiment with the initial condition $\phi_0(x) = \cos(x)$ and the variable velocity $u(x) = 2 + 3/2 \cos(x)$ computed with the general second-order scheme (3.1).

Secondly, we use $u(x) = 1 + 3/4 \cos(x)$ and the non-smooth initial condition given as follows:

$$\phi_0(x) = 2 \arcsin(\sin(x + \pi/2))/\pi. \quad (4.1)$$

The exact solution to the described example is

$$\phi(x, t) = \frac{2}{\pi} \arcsin \left(\cos \left(2 \arctan \left(\sqrt{7} \tan \left(\sqrt{7}/8 \left(t - 8 \arctan \left(\frac{\tan(x/2)}{\sqrt{7}} \right) / \sqrt{7} \right) \right) \right) \right) \right).$$

The computational domain is $x \in [-\pi/2, 3\pi/2]$ and $t \in [0, 8\pi/\sqrt{7}]$. The chosen settings lead to Courant numbers C_i that range from approximately 0.43 to 3. The results can be seen in Figure 4.2 and Table 4.4. Again, the direct scheme gives slightly better accuracy for the approximation of ϕ , but exhibits oscillatory behavior for the approximation of $\partial_x \phi$.

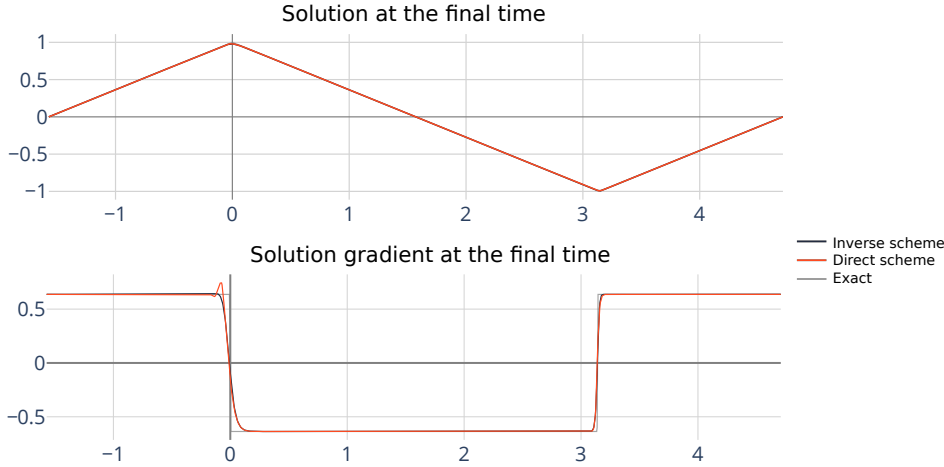


FIG. 4.2. Numerical solutions at the final time $T = 8\pi/\sqrt{7}$ of the advection equation with variable velocity and the initial condition (4.1) computed with the direct scheme (1.4) and the general scheme (3.1).

I	N	Direct scheme				General scheme			
		E_l^N	EOC	E_∞	EOC	E_l^N	EOC	E_∞	EOC
100	10	8.86E-01		5.00E-01		1.79E+00		4.75E-01	
200	20	3.45E-01	1.36	3.14E-01	0.67	6.69E-01	1.42	2.92E-01	0.70
400	40	1.26E-01	1.46	1.87E-01	0.74	2.37E-01	1.49	1.73E-01	0.75
800	80	4.43E-02	1.50	1.10E-01	0.77	8.35E-02	1.51	1.02E-01	0.76
1600	160	1.57E-02	1.50	6.52E-02	0.75	2.94E-02	1.50	6.08E-02	0.75

TABLE 4.4

Accuracy results for numerical experiment with the initial condition (4.1) and the variable velocity $u(x) = 1 + 3/4 \cos(x)$ computed with the direct scheme (1.4) and the general second-order scheme (3.1).

5. Conclusion. In this paper, we introduced a novel non-traditional second-order accurate finite-difference scheme tailored to solve the representative advection equation (1.1). Our primary objective was to explore alternative strategies for avoiding non-physical oscillations in the gradient of numerical solution without resorting to the limiting in time towards the first-order accurate scheme.

Using the inverse Lax-Wendroff procedure, we derived the inverse scheme (2.7) that incorporates numerical values at future time points. Together with the WENO parameters (2.8), the scheme is second-order accurate for smooth solutions, and it is essentially non-oscillatory in general for the maximal Courant number larger than one. Applying this scheme using the marching in space and the fast sweeping method, the numerical values are obtained explicitly.

Furthermore, to apply the inverse scheme using the traditional marching in time, we extended it with the predictor-corrector approach (2.10) by using the predicted values computed with the first-order accurate method. A similar approach is used to define extended backward differentiation formulae in [3] to solve ODEs numerically. Finally, we introduced the general second-order accurate scheme capable of delivering results without any oscillations across all Courant number values without limiting to the first-order scheme.

The numerical schemes are formulated in one dimension and applied in several numerical experiments with the sole purpose of demonstrating some advantages when considering discretization methods with predicted values of the solution at future time points. We plan to investigate such types of numerical scheme in more general cases, not necessary derived only with the inverse Lax-Wendroff procedure.

REFERENCES

- [1] Antonio Baeza, Raimund Bürger, María Martí, Pep Mulet, and David Zorío. On approximate implicit Taylor methods for ordinary differential equations. *Comp. Appl. Math.*, 39(4):304, October 2020.
- [2] Jeff Bezanson, Alan Edelman, Stefan Karpinski, and Viral B Shah. Julia: A fresh approach to numerical computing. *SIAM review*, 59(1):65–98, 2017.
- [3] J. R. Cash. On the integration of stiff systems of O.D.E.s using extended backward differentiation formulae. *Numerische Mathematik*, 34(3):235–246, September 1980.
- [4] Stéphane Clain, Gaspar J Machado, and Maria Teresa Malheiro. Compact schemes in time with applications to partial differential equations. *Computers & Mathematics with Applications*, 140:107–125, 2023.
- [5] Karthikeyan Duraisamy and James D. Baeder. Implicit scheme for hyperbolic conservation laws using nonoscillatory reconstruction in space and time. *SIAM J. Sci. Comput.*, 29(6):2607–2620, January 2007.
- [6] Peter Frolkovič, Svetlana Křišková, Michaela Rohová, and Michal Žeravý. Semi-implicit methods for advection equations with explicit forms of numerical solution. *Japan J. Indust. Appl. Math.*, 39:843–867, 2022.
- [7] Peter Frolkovič and Michal Žeravý. High resolution compact implicit numerical scheme for conservation laws. *Applied Mathematics and Computation*, 442:127720, 2023.
- [8] Peter Frolkovič and Nikola Gajdošová. Unconditionally stable higher order semi-implicit level set method for advection equations. *Applied Mathematics and Computation*, 466:128460, April 2024.
- [9] Friedemann Kemm. A comparative study of TVD-limiters—well-known limiters and an introduction of new ones. *Int. Journal for Numerical Methods in Fluids*, 67(4):404–440, 2011.
- [10] Chang Ho Kim, Youngsoo Ha, Hyoseon Yang, and Jungho Yoon. A third-order WENO scheme based on exponential polynomials for Hamilton-Jacobi equations. *Appl. Num. Math.*, 165:167–183, 2021.
- [11] Randall J Leveque. *Finite Volume Methods for Hyperbolic Problems*. Cambridge UP, 2004.
- [12] Gabriella Puppo, Matteo Semplice, and Giuseppe Visconti. Quinpi: Integrating conservation laws with CWENO implicit methods. *Commun. Appl. Math. Comput.*, February 2022.
- [13] Jianxian Qiu and Chi-Wang Shu. Hermite WENO schemes for Hamilton-Jacobi equations. *J. Comput. Phys.*, 204(1):82–99, 2005.
- [14] James Sethian. *Level Set Methods and Fast Marching Methods*. Cambridge UP, 1999.
- [15] Chi-Wang Shu. Essentially non-oscillatory and weighted essentially non-oscillatory schemes for hyperbolic conservation laws. In *Advanced Numerical Approximation of Nonlinear Hyperbolic Equations*, Lecture Notes in Mathematics, pages 325–432. Springer, Berlin, Heidelberg, 1998.
- [16] Chi-Wang Shu. Inverse Lax-Wendroff Boundary Treatment: a Survey. *Communications in Mathematical Research*, 38(3):18, 2022.
- [17] Jonas Zeifang and Jochen Schütz. Implicit two-derivative deferred correction time discretization for the discontinuous Galerkin method. *Journal of Computational Physics*, page 111353, 2022.
- [18] Hongkai Zhao. A fast sweeping method for eikonal equations. *Math. Comput.*, 74(250):603–627, 2005.